Molecular Biology of the Cell
Vol. 15, 982–989, March 2004

# Nonmuscle Myosin IIB Is Involved in the Guidance of Fibroblast Migration[V]

**Chun-Min Lo,* Denis B. Buxton,† Gregory C.H. Chua,* Micah Dembo,‡ Robert S. Adelstein,† and Yu-Li Wang*§**

*Department of Physiology, University of Massachusetts Medical School, Worcester, Massachusetts 01605; †Laboratory of Molecular Cardiology, National Heart, Lung, and Blood Institute, National Institutes of Health, Bethesada, Maryland 20892; and ‡Department of Biomedical Engineering, Boston University, Boston, Massachusetts 02215

Submitted June 4, 2003; Revised October 28, 2003; Accepted November 13, 2003
Monitoring Editor: Paul Matsudaira

**Although myosin II is known to play an important role in cell migration, little is known about its specific functions. We have addressed the function of one of the isoforms of myosin II, myosin IIB, by analyzing the movement and mechanical characteristics of fibroblasts where this protein has been ablated by gene disruption. Myosin IIB null cells displayed multiple unstable and disorganized protrusions, although they were still able to generate a large fraction of traction forces when cultured on flexible polyacrylamide substrates. However, the traction forces were highly disorganized relative to the direction of cell migration. Analysis of cell migration patterns indicated an increase in speed and decrease in persistence, which were likely responsible for the defects in directional movements as demonstrated with Boyden chambers. In addition, unlike control cells, mutant cells failed to respond to mechanical signals such as compressing forces and changes in substrate rigidity. Immunofluorescence staining indicated that myosin IIB was localized preferentially along stress fibers in the interior region of the cell. Our results suggest that myosin IIB is involved not in propelling but in directing the cell movement, by coordinating protrusive activities and stabilizing the cell polarity.**

## INTRODUCTION

The functional roles of myosin II in nonmuscle cells have been an important topic of investigation. Although its involvement in cytokinesis has been investigated in detail (Robinson and Spudich, 2000), there is also strong evidence that myosin II plays a role in cell migration. For example, although myosin II null mutants of *Dictyostelium* are capable of migration, they display a lower migration speed and a loss of forward bias in protrusion compared with wild-type cells (Wessels *et al*., 1988), particularly on surfaces of increased adhesiveness (Jay *et al*., 1995).

Fibroblast migration involves a number of controlled and coordinated processes, including protrusion, adhesion, translocation, and detachment (Lauffenburger and Horwitz, 1996; Mitchison and Cramer, 1996; Sheetz *et al*., 1998). It is commonly accepted that translocation of the cell body and detachment from the substrate require contractile forces (Jay *et al*., 1995; Wolenski, 1995; Anderson *et al*., 1996; Svitkina *et al*., 1997). Consistent with the idea, treatment of cells with myosin II inhibitors causes relaxation of traction forces and impairment of cell migration (Pelham and Wang, 1999). Equally important is a guidance mechanism in response to environmental cues. In addition to chemotaxis, fibroblasts show profound responses in morphology, traction forces, and motility rates, to physical signals (Pelham and Wang, 1997; Lo *et al*., 2000). They are also able to steer their migration toward substrates of high rigidity (Lo *et al*., 2000). Because the detection of such physical characteristics as rigidity cannot be achieved through purely chemical means, the cell must invoke a contractile mechanism that probes the environment. Myosin II may be involved in such a sensing structure at focal adhesions (Burridge and Chrzanowska-Wodnicka. 1996) and/or in the transduction of extracellular physical cues into intracellular chemical signals.

There are three known nonmuscle myosin II isoforms, referred to as myosin IIA, myosin IIB, and myosin IIC, respectively, in vertebrates (Katsuragawa *et al*., 1989; Simons *et al*., 1991; Berg *et al*., 2001; Golomb *et al*., 2004). Myosin IIA and IIB are expressed in a variety of cultured cells, whereas myosin IIC may be induced during hemopoietic differentiation (Buxton *et al*., 2003). The differential localization of myosins IIA and IIB suggests that they are involved in distinct functions (Maupin *et al*., 1994; Rochlin *et al*., 1995; Kelley *et al*., 1996; Kolega, 1998). In migrating endothelial cells, myosin IIB was enriched at the trailing region, whereas myosin IIA was found preferentially toward the leading edge (Kolega, 1998). In contrast, myosin IIB was localized at the leading edge of *Xenopus* A6 cells, whereas myosin IIA was present along fibrillar structures in the more interior cytoplasm (Kelley *et al*., 1996).

A more direct way to test the function of myosin II isoforms is to disrupt the expression or function of the proteins through targeted gene ablation. Ablation of nonmuscle myosin IIB gene in mice causes defects in cardiac and neuronal development (Tullio *et al*., 1997). Although the defects are possibly associated with impaired cell migration, the exact cellular basis is unclear. To understand how myosin IIB

Article published online ahead of print. Mol. Biol. Cell 10.1091/mbc.E03–06–0359. Article and publication date are available at www.molbiolcell.org/cgi/doi/10.1091/mbc.E03–06–0359.

[V] Online version of this article contains supplementary video material for some figures. Online version is available at www.molbiolcell.org.

§ Corresponding author. E-mail address: yuli.wang@umassmed.edu.

participates in cell migration, we have investigated the movement and mechanical characteristics of mouse embryonic fibroblasts lacking nonmuscle myosin IIB. The response of these cells to mechanical stimuli was further probed using polyacrylamide flexible substrates. Our results indicate that the main defect of myosin IIB null cells was not the rate of migration or the generation of traction forces, but the directional stability of migration and the ability to respond to mechanical stimulation. We suggest that nonmuscle myosin IIB plays an important role in steering and stabilizing the polarity of cell migration.

## MATERIALS AND METHODS

### *Polyacrylamide Substrates and Cell Culture*

Myosin IIB null and control mouse embryonic fibroblasts were derived by explanting and culturing day 13 embryos after removing the head and internal organs. Cells were maintained at 37°C and 5% $CO_2$ in DMEM (Sigma-Aldrich, St. Louis, MO), supplemented with 10% fetal bovine serum (JRH Biosciences, Lenexa, KS), 2 mM L-glutamine, 50 $\mu$g/ml streptomycin, 50 U/ml penicillin, and 250 ng/ml amphotericin B (Invitrogen, Carlsbad, CA).

The general method for preparing polyacrylamide substrate has been described previously (Wang and Pelham, 1998). The substrates contain 5% total acrylamide and either 0.1% (for stiff substrates) or 0.06% bis-acrylamide (for soft substrates). The flexibility of polymerized sheets was determined as described previously (Lo *et al*., 2000). The Young's modulus of substrates with 0.1 and 0.06% bis-acrylamide was estimated as 28 and 15 kNt/m$^2$, respectively. Measurements of traction forces were limited to isolated, well spread/extended cells (e.g., excluding mitotic cells) that fit within the central region of the imaging field (~60 $\mu$m). To apply local mechanical strain to the flexible substrate, the tip of a blunted microneedle was gently lowered onto the surface with a micromanipulator, and the substrate was deformed by pushing the needle toward the leading edge of a migrating cell (Lo *et al*., 2000). Cells that showed immediate shortening in response to the substrate deformation were included in the analysis. Positive response was defined as the retraction of protrusions proximal to the needle and the expansion of protrusions distal to the needle. This caused the cell to change its direction of migration.

Rescue of myosin IIB knockout cells were performed by expressing green fluorescent protein (GFP)-tagged constructs of myosin IIB or IIA (constructs kindly supplied by Dr. Qize Wei, National Institutes of Health, Bethesda, MD). Transfection was carried out with a Nucleofector machine (Amaxa, Gaithersburg, MD) and 4.5 $\mu$g of DNA, by using program T20 and kit V.

### *Immunofluorescence Staining*

For immunofluorescence staining of vinculin, cells were washed with 37°C phosphate-buffered saline (PBS) and fixed with 4% formaldehyde (Electron Microscopy Sciences, Ft. Washington, PA), in PBS containing 0.1% Triton X-100 (Roche Diagnostics, Mannheim, Germany) at 37°C for 10 min as described previously (Pelham and Wang, 1997). Monoclonal anti-vinculin antibodies were obtained from Sigma-Aldrich (clone VIN-11-5) and used at a dilution of 1:100. Alexa-546–conjugated goat anti-mouse secondary antibodies were obtained from Molecular Probes (Eugene, OR) and used at a dilution of 1:100.

For immunofluorescence staining of myosin IIA and myosin IIB, cells were washed with 37°C PBS and fixed with a mixture of 0.1% glutaraldehyde (Polysciences, Warrington, PA) and 1.0% formaldehyde in cytoskeleton buffer containing 0.3% Triton X-100 (Small, 1981) at 37°C for 1 min and then postfixed with 0.5% glutaraldehyde in 37°C cytoskeleton buffer for 15 min (O'Connell *et al*., 1999). Staining was performed using polyclonal antibodies specific for the C-terminal region of MHC-A or MHC-B, at a dilution of 1:100. Alexa-546–conjugated anti-rabbit IgG secondary antibodies were purchased from Molecular Probes and used at a dilution of 1:100. Actin filaments were stained with Alexa-488–phalloidin (Molecular Probes) following manufacturer's protocol.

### *Cell Migration Assays*

Experiments were performed 15 h after plating the cells on coverglass or polyacrylamide substrates at a low density. Phase contrast images were recorded using a cooled charge-coupled device camera (TE/CCD-576EM; Princeton Instruments, Trenton, NJ), attached to an IM-35 microscope (Carl Zeiss, Jena, Germany) equipped with a 40×, numerical aperture (NA) 0.65 Achromat phase objective lens and a stage incubator. The position of the cell was determined every 2 min for a period of 50–80 min, based on the center of the nucleus. Migration speed (S) and directional persistence (P) were calculated based on the persistent random walk equation $<d^2(t)> = 2S^2P[t - P(1 - e^{-t/P})]$, where $<d^2(t)>$ is the mean squared displacement (Dunn, 1983). Migration speed was estimated from double reciprocal plots of the square root of $<d^2(t)>$ against t (as 1/slope), and directional persistence was estimated as slope/6 multiplied by the y-intercept. Persistent distance was calculated as S*P. The instantaneous direction of cell migration was determined by connecting the center of nucleus at consecutive time points.

Modified Boyden chamber assay was performed in serum-free media CCM1 (Hyclone Laboratories, Salt Lake City, UT) by using Transwell polycarbonate membrane (1.1-cm$^2$ surface area, 12-$\mu$m pore size; Costar, Cambridge, MA). The membrane surface facing the lower chamber was coated by incubating with 40 $\mu$g/ml type I collagen or 20 $\mu$g/ml fibronectin for 2 h at 37°C. Fifteen hours after adding $10^5$ cells to the upper chamber, cells remaining on the upper surface of the membrane were gently removed with a cotton swab. Cells migrated onto the lower membrane surface were fixed and stained with 1 mg/ml propidium iodide. Cell number in 10 randomly chosen fields was counted and averaged, by using a 10× NA 0.25 Achromat phase objective. To measure the corresponding rate of random migration, the same procedure was applied to membranes coated on both sides with collagen or fibronectin.

In the wound healing assay, confluent monolayers were scratched with the tip of a plastic pipette, and images were recorded for a period of 24 h by using a 10× NA 0.25 Achromat phase objective. The rate of wound closure was calculated by measuring the distance between the two wound edges at 0 and at 4 h and dividing by the time interval (4 h). The measurements were carried out at one or two different points for each wound.

### *Determination of Traction Forces and Cell Spreading Area*

Traction forces generated by the cell were determined essentially as described previously (Dembo and Wang, 1999). Briefly, deformation of the substrate due to cell-generated forces was detected based on the displacement of embedded fluorescent beads near the substrate surface. Images of beads were recorded before and after cell detachment with 0.05% trypsin. After registration of the images, a map of displacement vectors was generated using custom software (Marganski *et al*., 2003). Calculation of traction forces was carried out using the displacement vectors, the cell boundary, the Young's modulus and the Poisson's ratio as the input (Dembo and Wang, 1999). Total mechanical output was calculated by multiplying the average traction stress by the surface area of the cell, which was measured by counting the number of image pixels within the cell boundary by using custom software. Angular distribution of traction forces was analyzed by integrating the positive projected magnitude of traction stress at each pixel along different directions. As the net force is always set to zero during computation, only positive magnitudes were used for the integration.

## RESULTS

### *Morphology and Migration of Myosin IIB Null Cells*

A stable line of myosin IIB null fibroblasts was prepared from mouse embryo in which myosin IIB had been ablated (Tullio *et al*., 1997). A control cell line, prepared from homozygous wild-type littermates, was selected based on its expression of a similar level of nonmuscle myosin IIA as in myosin IIB null cells. Neither cell line expressed a detectable amount of myosin IIC (Buxton and Adelstein, unpublished observations). The only detectable difference in protein composition between the myosin IIB null and control cells was the absence of myosin IIB heavy chains in null cells.

Unlike control cells (Figure 1A and Video 1), and other normal fibroblasts such as NIH3T3 cells, a large percentage of myosin IIB null cells developed long processes and multiple, unstable protrusions when plated at a low density (~75%, n = 424; Figure 1B and Video 2, Figure 1C and Video 3). Most of these processes collapsed suddenly toward the cell body (Figure 1C, short arrows; and Video 3), whereas others broke off, leaving behind small pieces of motile cytoplasm (Figure 1C, arrowheads; and Video 3). Time-lapse analysis indicated that these protrusions lasted on average 40 min, in contrast to 100 min for the lamellipodia in control cells. Consistent with the instability of protrusions, mutant cells showed rapid changes in cell shape and switched their direction of migration at a high frequency (Figure 1B, arrows; and Video 2).

To confirm that the deficiency of myosin IIB is responsible for the change in morphology, we have expressed GFP-myosin IIB in myosin IIB null cells. GFP signals were found to localize along stress fibers (Figure 2A). All the 10 GFP-positive cells showed a normal morphology and no random

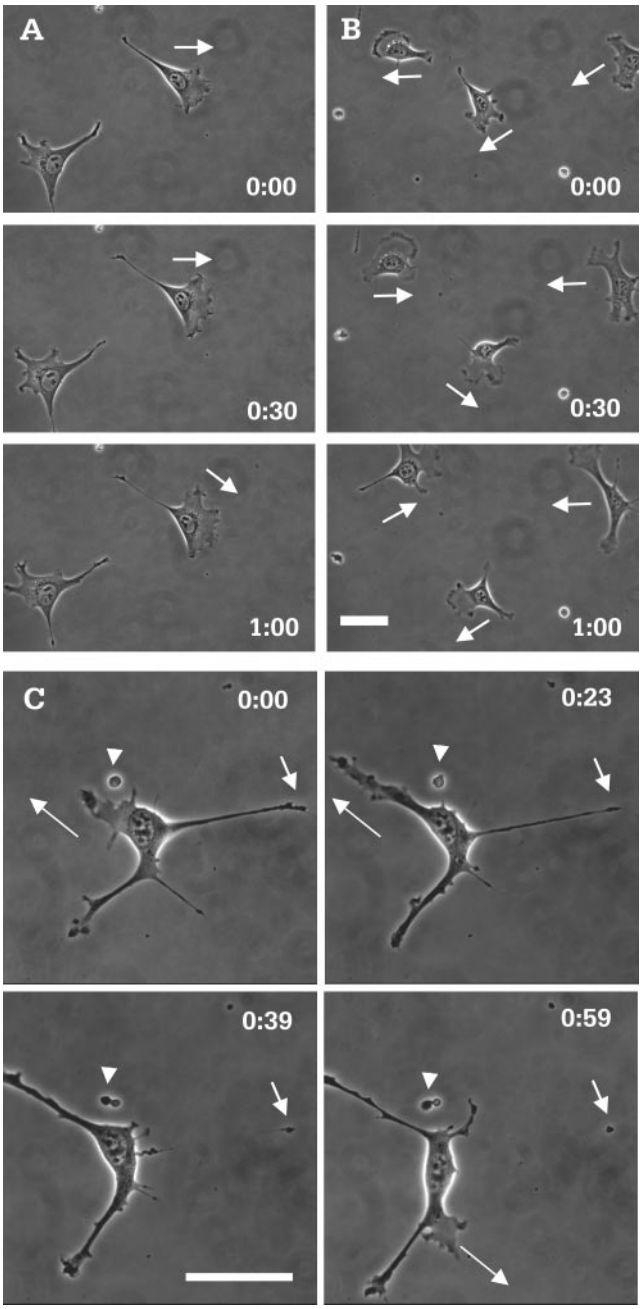


**Figure 1.** Morphology and migratory behavior of control and myosin IIB null cells. Although most control cells maintained their morphology over a 60-min period (A), mutant cells showed rapid changes in cell shape during the same period of time (B). In addition mutant cells migrate with a highly unstable polarity (B, arrows), compared with control cells (A, arrows). Images of high magnification show protrusion, elongation (C, long arrows), and rapid retraction of processes (C, short arrows). The latter creates small pieces of motile cytoplasm that litter the glass surface (C, arrowheads). Time in hours and minutes is indicated in each image. Bar, 50 $\mu$m.

protrusive activities (Figure 2, B and C). In contrast, 8 of 11 cells transfected with GFP-myosin IIA showed an irregular morphology as for untransfected mutant cells (Figure 2, D and E).

The migration of control and myosin IIB null cells was analyzed quantitatively based on mean squared displacement of 11 control and 17 mutant cells (Dunn, 1983). As seen in Figure 3, double reciprocal plots of mean square displacement against elapsed time indicated that mutant cells migrated with a higher speed but a reduced directional persistence than did control cells (Table 1), i.e., myosin IIB null cells showed a higher frequency of turning. The combination of higher speed and lower persistence resulted in a similar persistent distance between mutant and control cells, indicating that myosin IIB null and control cells migrated for a similar distance before turning. However, the faster pace made the mutant cells seem much more unstable.

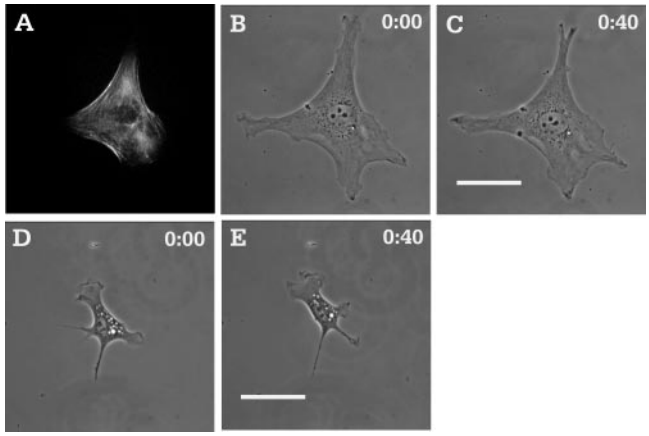


**Figure 2.** Restoration of normal morphology of myosin IIB mutant cells by the reexpression of GFP-myosin IIB. Myosin IIB nulls were transfected with a vector carrying the sequence of GFP-myosin IIB. GFP signals were found along stress fibers (A). Cells expressing GFP-myosin IIB show a normal morphology and no random protrusive activities (B and C). In contrast, cells expressing GFP-myosin IIA maintained the irregular, unstable morphology as for the original myosin IIB null cells (D and E). Time in hours and minutes is indicated. Bar, 50 $\mu$m.

### *Myosin IIB Null Cells Are Defective in Directional Movement*

The reduced directional persistence suggested that myosin IIB cells might not be able to maintain a stable direction during targeted migration such as haptotaxis. We therefore

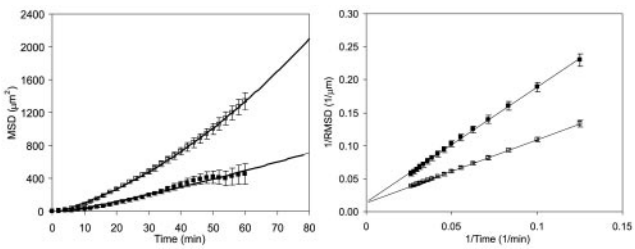


**Figure 3.** Quantitative analysis of cell migration. Plotting of mean squared distance against time (from 11 control cells and 17 mutant cells; each data point represents a mean ± SEM) indicates that mutant cells (A, open square) are able to migrate over a longer distance than do control cells (A, solid square), irrespective of the direction. However, double reciprocal plot of root mean squared distance against time, where migration speed is calculated as 1/slope and directional persistence is calculated as slope/6× y-intercept, indicates that mutant cells (B, open square) migrate at a higher speed but with a decreased persistence compared with control cells (B, solid square; Table 1).

**Table 1.** Average migration speed and persistence time of control and myosin IIB null cells cultured on glass

| | Control | Myosin IIB null |
|---|---|---|
| Speed ($\mu$m/min) | 0.57 ± 0.23 (n = 11) | 1.04 ± 0.11 (n = 17) |
| Persistence (min) | 20.12 ± 2.88 (n = 11) | 12.56 ± 2.02 (n = 17) |
| Persistent distance ($\mu$m) | 11.46 | 13.06 |

Positions of the cell were determined every 2 min by using time-lapse phase microscopy. Migration speed and persistence were calculated from double reciprocal plots of root mean square displacements against time as described in MATERIALS AND METHODS. Persistent distance was calculated by multiplying mean speed with mean persistence. Values shown are mean ± standard error.

tested the cell behavior with a modified Boyden chamber assay. In this test, cells migrated from an uncoated surface of a porous membrane toward the opposite surface coated with extracellular matrix (haptotaxis). Membranes coated on both sides served as the reference (random migration). As seen in Figure 4, control cells showed a ratio of ~5 between haptotaxis and random migration on collagen-coated membrane and ~6 on fibronectin-coated membrane. In contrast, this ratio for myosin IIB null cells was close to 2 on collagen- and 1 on fibronectin-coated membrane. These results indicate that myosin IIB is required for haptotaxis.

A second test was to determine the ability of myosin IIB cells to cover a wound on the monolayer. Six independent observations were performed for both mutant and control cells. A typical example is shown in Figure 5A, where the cell-free area was covered completely by control cells in ~6 h. In contrast, only 60–70% of the open area was covered by mutant cells over the same period (Figure 5, B and C). However, at such high cell densities, mutant cells showed no apparent increase in unstable protrusions as seen for cells at a low density (Figure 1). The reduced rate of wound closure seemed to result from an increase in the resistance to forward migration due to cell-cell adhesion.

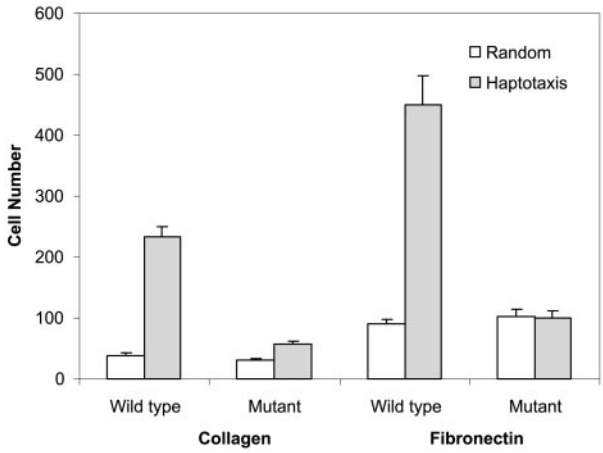


**Figure 4.** Haptotactic migration assay of control and myosin IIB mutant cells. To measure haptotactic movements, cells were plated on porous membrane with one side coated with collagen or fibronectin, at a concentration of 40 and 20 $\mu$g/ml, respectively. Random migration was measured by applying this coating to both sides of the membrane. The number of cells that migrated across the membrane was counted after 15 h. Bars represent the mean ± SE from six independent experiments. For either collagen or fibronectin coating, myosin IIB null cells show no significant haptotactic migration. To the contrary, control cells show a haptotaxis/random migration ratio of 5–6.

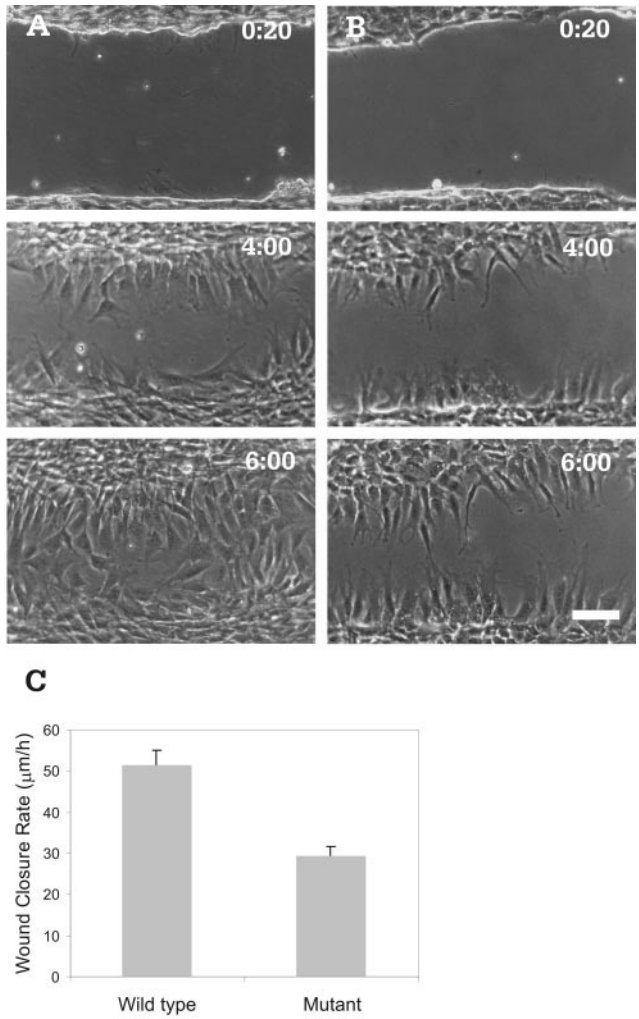


**Figure 5.** Wound-induced migration of control and myosin IIB null cells. Confluent monolayers of either control (A) or myosin IIB null (B) cells were wounded at time 0. Control cells migrate and cover the cell-free area in ~6 h, whereas mutant cells cover only about two-thirds of the area over the same period. Hours and minutes since the wound are indicated in each image. Bar, 100 $\mu$m. Average rates of wound closure during the first 4 h of repair were calculated from six independent experiments (C). Error bars indicate SE of the mean.

### *Myosin IIB Null Cells Are Defective in the Organization of Traction Forces and in Sensing Mechanical Signals*

We have previously proposed a force-dependent mechanism for cells to respond to external physical signals (Lo *et al.*, 2000). To investigate the possible involvement of myosin IIB in generating traction forces and in detecting substrate rigidity, cells were cultured on flexible polyacrylamide substrates coated with type 1 collagen. Despite the ablation of myosin IIB, null cells maintained ~75% of the total mechanical output compared with control cells. As for control cells (Figure 6A) and 3T3 fibroblasts (Dembo and Wang, 1999),

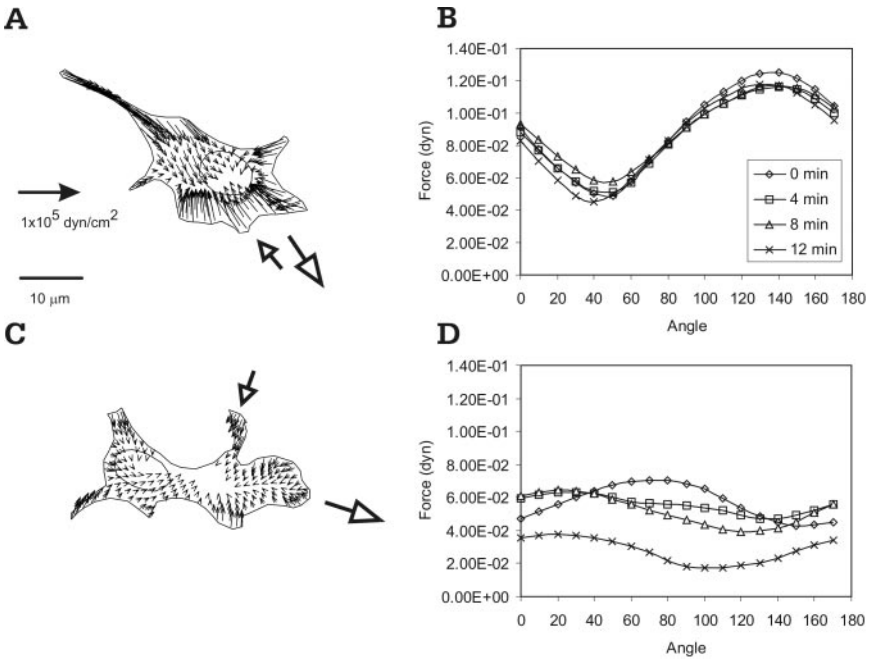


**Figure 6.** Traction forces generated by control (A and B) and myosin IIB null cells (C and D). Cells were plated on flexible substrates embedded with beads. The distribution of traction stress was calculated based on the displacements of beads and rendered as vector plots (A and C). Graphs show the corresponding angular distribution of traction forces at four time points (B and D). Control cells show a pattern of traction stress similar to that of 3T3 fibroblasts (A), with strong traction forces concentrated at the leading edge. The direction of maximal traction force (A, short hollow arrow) is antiparallel to the direction of cell migration (A, long hollow arrow) and is 90° from the direction of minimal traction forces (B). In contrast, mutant cells show an unstable, poorly defined direction of maximal traction forces (C, short hollow arrow; D), which bears no apparent relationship to either the direction of cell migration (C, long hollow arrow) or the direction of minimal traction force (D).

strong inward traction forces were concentrated at protrusive or ruffling regions of myosin IIB null cells (Figure 6C).

We showed previously that for 3T3 cells, the direction of maximal traction forces remained antiparallel to the direction of cell migration (Munevar *et al*., 2001). This was confirmed with 52 measurements made during >2 h of two migrating control cells (Figure 6, A and B). In most cases, the magnitude of traction forces in control cells exhibited an apparently sinusoidal dependence on the angle, i.e., with symmetric peaks and valleys separated by 90° (observed in 52 of 72 measurements made with 22 cells; Figure 6B; see also Munevar *et al*., 2001). The exceptions were always associated with the reorientation of cell migration.

In contrast, the direction of maximal traction forces in mutant null cells was unstable, showing no consistent relationship to the direction of cell migration (based on 97 measurements made during >2 h of three cells; Figure 6, C and D). Less than 50% of the measurements showed an apparently sinusoid relationship between traction forces and the angle (57 of 121 measurements made with 27 cells). In addition, the angular dependence curve showed no well-defined peak or valley (Figure 6D), and the shape was highly variable.

As shown previously, normal fibroblasts responded to increasing substrate rigidity by increasing their spreading area and mechanical output (Lo *et al*., 2000; Table 2). In contrast, myosin IIB null cells showed no apparent response to substrate rigidity (Table 2). Furthermore, both 3T3 fibroblasts and control cells reoriented their migration away from pushing forces (Lo *et al*., 2000; observed with all of the eight 3T3 cells and eight control cells tested; Figure 7A and Video 4), whereas none of the seven myosin IIB null cells tested showed an apparent turning response to pushing forces (Figure 7B and Video 5).

### *Organization of Myosin and Vinculin in Control and Myosin IIB Null Cells*

Additional insights into the function of myosin IIB may be gained from the localization of IIA and IIB. Phalloidin staining of actin filaments showed the presence of similar stress fibers in myosin IIB null cells and control cells (Figure 8, B, E, and H). Staining of myosin IIA showed localization along stress fibers and the lateral cortex in both control and myosin IIB null cells (Figure 8, A and G). The stress fibers looked like arrays of discrete, punctate structures, and stress fibers in different regions showed a similar extent of myosin IIA localization relative to actin filaments (Figure 8, C and I).

In control cells, staining of myosin IIB seemed more continuous along stress fibers than did myosin IIA (Figure

**Table 2.** Force output and spreading area of control and myosin IIB null cells on substrates of different rigidity

| Young's modulus ($kNt/m^2$) | Total force output (dyne) | | Spreading area ($10^3$ $\mu m^2$) | |
|---|---|---|---|---|
| | Control | Myosin II-B null | Control | Myosin II-B null |
| 15 | 0.44 ± 0.03 (n = 18) | 0.44 ± 0.04 (n = 20) | 1.71 ± 0.10 (n = 10) | 1.74 ± 0.16 (n = 10) |
| 28 | 0.57 ± 0.06 (n = 18) | 0.41 ± 0.03 (n = 20) | 2.07 ± 0.20 (n = 9) | 1.65 ± 0.15 (n = 10) |

Total force output for each cell was calculated by multiplying the average traction stress with the cell area. For control cells, the force output on stiff substrates was higher than that on soft substrates ($p = 0.02$). No statistically significant difference was found for mutant cells on substrates of different rigidity. Values shown are mean ± standard error.

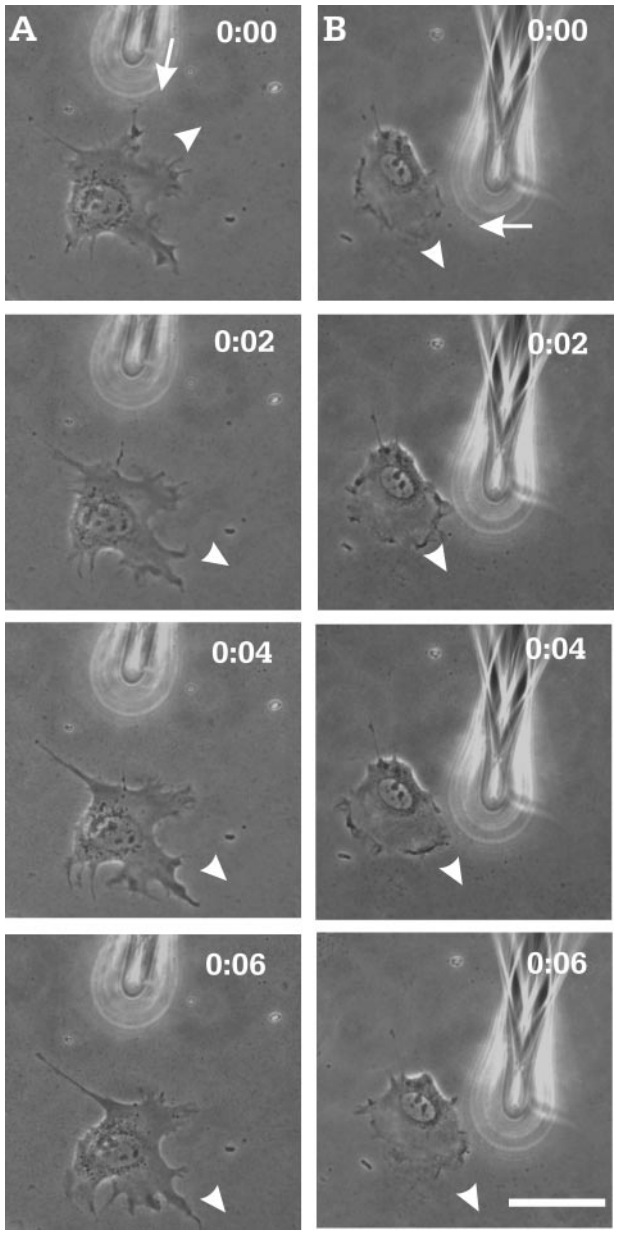


**Figure 7.** Response of myosin IIB null cells to local mechanical stimulations. A blunted microneedle was inserted into the polyacrylamide substrate near the lateral edge of a cell and then moved toward the cell to compress the substrate (arrows). The local change in substrate tension did not cause the mutant cell to change its direction of movement (B, arrowheads). However, similar manipulations caused control cells to move away from the needle (A, arrowheads). Hours and minutes since the beginning of the manipulation are indicated in each image. Bar, 50 $\mu$m.

8D). In addition, myosin IIB was localized preferentially along stress fibers in the central region of the cell (Figure 8, D and F). Neither myosin IIA nor IIB showed a concentration along the leading edge. As expected, immunofluorescence staining of the heavy chain of myosin IIB gave only background signals in null cells. Staining of vinculin showed qualitatively similar focal adhesions in both myosin IIB null and control cells (our unpublished data).

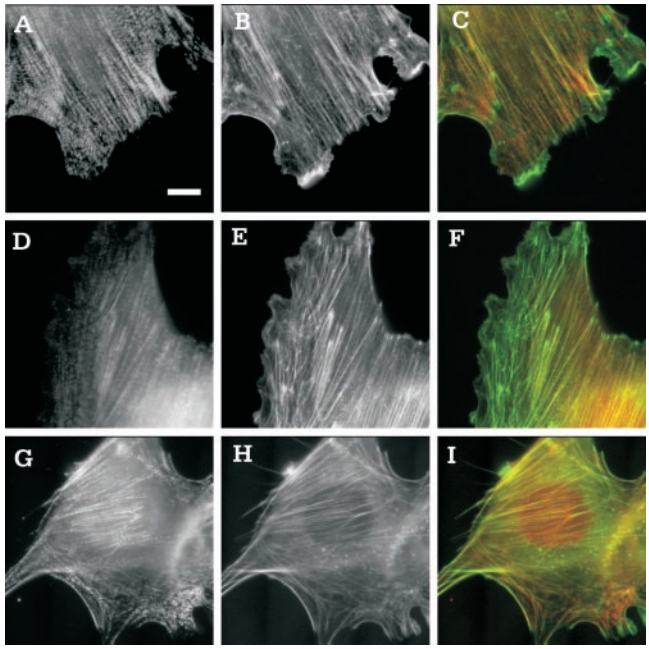


**Figure 8.** Organization of myosin IIA and IIB in control and myosin IIB null cells. Control cells (A–F) or myosin IIB null cells (G–I) were stained with antibodies against myosin IIA (A and G) or myosin IIB (D) and counterstained with fluorescent phalloidin (B, E, and H). Merged images of myosin and actin (C, F, and I) show regions enriched (more red) or depleted (more green) of the specific isoform of myosin. Myosin IIA seems to be more evenly distributed among stress fibers in central and peripheral regions (A–C and G–I), whereas myosin IIB is localized preferentially along stress fibers in the central region of control cells (D–F). Moreover, myosin IIA shows a more discrete punctate pattern along stress fibers than does myosin IIB (A and G). Bar, 10 $\mu$m.

## DISCUSSION

Recent studies have demonstrated strong, active mechanical interactions between migrating fibroblasts and the substrate, which likely serve not only to propel but also to guide cell migration (Munevar *et al*., 2001). Genetic and pharmacological manipulations indicated that myosin II plays an important role in these processes. For example, treatment of 3T3 fibroblasts with KT5926, an inhibitor of myosin light chain kinase, caused a dramatic reduction in traction forces and migration rate, without affecting the protrusion of the leading edge (Pelham and Wang, 1999). Similar treatments were found to inhibit uropod retraction, chemotaxis, and polarization of neutrophils (Eddy *et al*., 2000). Ablation of myosin II expression in *Dictyostelium* caused a similar defect in tail retraction and in the forward bias of pseudopod extension (Jay *et al*., 1995). Together, these observations suggested that myosin II may be required for regulating both frontal protrusion and tail retraction.

### *Defects of Myosin IIB Null Cells*

In this study, we addressed the functional role of nonmuscle myosin IIB in fibroblast migration by using cells derived from mouse embryos where the gene of myosin IIB heavy chain has been ablated (Tullio *et al*., 1997). The ability of these animals to develop to the neonatal stage and of the cells to grow in culture suggests that myosin IIA alone is sufficient for cytokinesis, one of the key functions of myosin II (Robinson and Spudich, 2000). However, the defects in

cardiac and neuronal development indicate that myosin IIB is required for some other significant functions (Uren *et al.*, 2000). Our initial speculation was that myosin IIB cells might be defective in their migration and/or mechanical output. To our surprise, myosin IIB null fibroblasts were not only capable of migration but also migrated at a higher raw speed than did control cells (Table 1 and Figure 3). In addition, myosin IIB null cells maintained most of the traction forces compared with control cells (Table 2 and Figure 6). Previous studies with myosin IIB-deficient neurons have also revealed substantial traction forces exerted by the filopodia (Bridgman *et al.*, 2001).

From the present observations, the most striking defect of myosin IIB null cells was their multiple, disorganized, and transient lamellipodia (Figure 1). This leads to an unstable polarity of migration, manifested quantitatively as a decrease in migratory persistence (Table 1 and Figures 1 and 3). In addition, although normal migrating fibroblasts maintained a stable direction of maximal traction forces antiparallel to the direction of cell migration (Munevar *et al.*, 2001), the multiple projections in myosin IIB nulls cells seemed to engage in a tug of war and could no longer define an unambiguous direction of cell migration (Figures 1C and 6). The loss of stable polarity may explain the defects of myosin IIB null cells in haptotaxis as seen in the modified Boyden chamber assay (Carter, 1967; Figure 4). Myosin IIB null cells also showed a delay in an in vitro wound healing assay (Figure 5), although this seemed to be caused by an increased resistance to forward migration at high cell densities. In addition, null cells showed no apparent response in traction forces and spreading areas to substrate rigidity (Table 2), and no detectable directional guidance by mechanical stimulations (Figure 7), indicating that they are defective in responding to mechanical signals. Similar defects may affect the behavior of neuronal growth cones, including unstable lamellipodia and increased retrograde flow of the actin cytoskeleton (Brown and Bridgman, 2002).

### *Functions of Myosin IIB in Cell Migration*

There are several possible ways that myosin IIB could contribute to cell migration. First, myosin IIB may be involved in the detection of mechanical signals. We argued previously that responses to such physical parameters as substrate rigidity must involve the application of contractile forces at adhesion sites, coupled to the transduction of mechanical feedback into chemical events (Pelham and Wang, 1997; Lo *et al.*, 2000). Myosin IIB may be responsible for generating such probing forces. Myosin was also suggested to mediate "inside-out" signaling, by promoting the assembly of stress fibers and focal adhesions from inside the cell in response to substrate adhesion and growth factors (Burridge and Chrzanowska-Wodnicka, 1996). Although we found no apparent defect in the distribution of vinculin, it is likely that focal adhesions are less stable in mutant cells than in control cells as suggested by their highly irregular behavior. The concentration of myosin IIB at the leading edge, as found in *Xenopus* A6 cells, is consistent with a role in membrane signaling (Kelley *et al.*, 1996). However, because different regions of the cells are linked mechanically by the cytoskeleton network, even forces generated in the central region, as suggested by the distribution of myosin IIB (Figure 8), may propagate easily to the cell periphery.

Second, our observations suggest that myosin IIB is involved the coordination of primary and secondary protrusions. During normal fibroblast migration, secondary protrusions were generated continuously along the lateral edges, although most of them disappeared shortly and were unable to compete with the primary lamellipodium. Myosin IIB may be involved in such coordination by promoting the retraction of secondary protrusions and allowing the cell to maintain a regular shape and stable direction of migration. A defect in retraction may also lead to increased resistance and reduced rate of wound closure, as seen with myosin IIB null cells (Figure 5). Based on immunolocalization (Rochlin *et al.*, 1995), myosin IIB has also been speculated to play a role in the retraction of neuronal growth cone.

Third, myosin IIB may stabilize the direction of cell migration. Myosin IIB was found to mediate the anterior localization of $\beta$-actin mRNA (Latham *et al.*, 2001), despite its preferential localization along stress fibers in the central region of the cell (Figure 8). The localization of $\beta$-actin mRNA may in turn play a role in the stabilization of protrusion (Shestakova *et al.*, 2001). It is also possible that, through its preferential association with mature stress fibers in the central region, myosin IIB stabilizes the direction of cell migration. The distinct function of central stress fibers has also been suggested based on their different sensitivity to drugs against the Rho-dependent kinase and myosin light chain kinase from peripheral stress fibers (Totsukawa *et al.*, 2000; Katoh *et al.*, 2001).

### *Differential Functions of Myosin IIA and Myosin IIB*

Previous studies with antisense technologies and dominant negative constructs suggested that myosin IIA may be involved in cell adhesion and cell shape (Wei and Adelstein, 2000; Wylie and Chantler, 2001), whereas myosin IIB is essential for maintaining a normal growth cone mobility (Wylie *et al.*, 1998; Bridgman *et al.*, 2001). We found that myosin IIB null cells are able to maintain ~75% of the traction forces as detected in control cells, which contained a similar amount of myosin IIA in addition to a roughly equal amount of myosin IIB (our unpublished observations). Therefore, the relative contribution of myosin IIA to total traction forces should be three times higher than that of IIB. Interestingly, myosin IIA also showed two- to threefold higher activities than myosin IIB in both the actin-activated ATPase assay and in vitro motility assay (Kelley *et al.*, 1996).

A second prominent difference between the two myosin II isoforms is that myosin IIA is organized as sarcomere-like structures along stress fibers throughout the cell, whereas myosin IIB seemed to be more continuously distributed along stress fibers in the interior region (Figure 8). A similar differential distribution was described in previous studies with endothelial cells (Kolega, 1998), melanoma cells (Maupin *et al.*, 1994), nonneuronal gangalial cells (Rochlin *et al.*, 1995), and fibroblasts (Saitoh *et al.*, 2001). Together, these observations support the idea that myosin IIA is involved in a contractile function as in muscles (Figure 8), whereas myosin IIB may play primarily a regulatory role.

## ACKNOWLEDGMENTS

This work was funded by National Institutes of Health grant GM-32476 and National Aeronautics and Space Administration grant NAG 2-1245 to Y.-L.W., and National Institutes of Health grant GM-61806 to M.D.

## REFERENCES

Anderson, K.I., Wang, Y.-L., and Small, J.V. (1996). Coordination of protrusion and translocation of the keratocyte involves rolling of the cell body. J. Cell Biol. *134*, 1209–1218.

Berg, J.S., Powell, B.C., and Cheney, R.E. (2001). A millennial myosin census. Mol. Biol. Cell *12*, 780–94.

Bridgman, P.C., Dave, S., Asnes, C.F., Tullio, A.N., and Adelstein, R.S. (2001). Myosin IIB is required for growth cone motility. J. Neurosci. *21*, 6159–6169.

Brown, M.E., and Bridgman, P.C. (2002). Retrograde flow rate is increased in growth cones from myosin IIB knockout mice. J. Cell Sci. *116*, 1087–1094.

Burridge, K., and Chrzanowska-Wodnicka, M. (1996). Focal adhesions, contractility, and signaling. Annu. Rev. Cell. Dev. Biol. *12*, 463–518.

Buxton, D.B., Golomb, E., and Adelstein, R.S. (2003). Induction of nonmuscle myosin heavy chain II-C by butyrate in RAW 264.7 mouse macrophages. J. Biol. Chem. *278*, *15*, 449–455.

Carter, S.B. (1967). Haptotaxis and the mechanism of cell motility. Nature *213*, 256–260.

Dembo, M., and Wang, Y.-L. (1999). Stresses at the cell-to-substrate interface during locomotion of fibroblasts. Biophys. J. *76*, 2307–2316.

Dunn, G.A. (1983). Characterising a kinesis response: time averaged measures of cell speed and directional persistence. Agents Actions (suppl) *12*, 14–33.

Eddy, R.J., Pierini, L.M., Matsumura, F., and Maxfield, F.R. (2000). $Ca^{2+}$-dependent myosin II activation is required for uropod retraction during neutrophil migration. J. Cell Sci. *113*, 1287–1298.

Golomb, E., Ma, X., Jama, S.S., Preston, Y.A., Kawamoto, S., Shoham, N.G., Goldin, E., Conti, M.A., Sellers, J.R., and Adelstein, R.S. (2004). Identification and clonacterization of nonmuscle myosin II-C, a new member of the myosin II family. J. Biol. Chem. *279*, 2800–2808.

Jay, P.Y., Pham, P.A., Wong, S.A., and Elson, E.L. (1995). A mechanical function of myosin II in cell motility. J. Cell Sci. *108*, 387–393.

Katoh, K., Kano, Y., Amano, M., Kaibuchi, K., and Fujiwara, K. (2001). Stress fiber organization regulated by MLCK and Rho-kinase in cultured human fibroblasts. Am. J. Physiol. *280*, C1669–C1679.

Katsuragawa, Y., Yanagisawa, M., Inoue, A., and Masaki, T. (1989). Two distinct nonmuscle myosin-heavy-chain mRNAs are differentially expressed in various chicken tissues. Eur. J. Biochem. *184*, 611–616.

Kelley, C.A., Sellers, J.R., Gard, D.L., Bui, D., Adelstein, R.S., and Baines, I.C. (1996). Xenopus nonmuscle myosin heavy chain isoforms have different subcellular localizations and enzymatic activities. J. Cell Biol. *134*, 675–687.

Kolega, J. (1998). Cytoplasmic dynamics of myosin IIA and IIB: spatial 'sorting' of isoforms in locomoting cells. J. Cell Sci. *111*, 2085–2095.

Latham, V.M., Yu, E.H., Tullio, A.N., Adelstein, R.S., and Singer, R.H. (2001). A Rho-dependent signaling pathway operating through myosin localizes $\beta$-actin mRNA in fibroblasts. Curr. Biol. *11*, 1010–1016.

Lauffenburger, D.A., and Horwitz, A.F. (1996). Cell migration: a physically integrated molecular process. Cell *84*, 359–369.

Lo, C.-M., Wang, H.-B., Dembo, M., and Wang, Y.-L. (2000). Cell movement is guided by the rigidity of the substrate. Biophys. J. *79*, 144–152.

Maupin, P., Phillips, C.L., Adelstein, R.S., and Pollard, T.D. (1994). Differential localization of myosin-II isozymes in human cultured cells and blood cells. J. Cell Sci. *107*, 3077–3090.

Mitchison, T.J., and Cramer, L.P. (1996). Actin-based cell motility and cell locomotion. Cell *84*, 371–379.

Marganski, W.A., Dembo, M., and Wang, Y.-L. (2003). Measurements of cell-generated deformations on flexible substrata using correlation-based optical flow. Methods Enzymol. *361*, 197–211.

Munevar, S., Wang, Y.-L., and Dembo, M. (2001). Traction force microscopy of migrating normal and H-ras transformed 3T3 fibroblasts. Biophys. J. *80*, 1744–1757.

O'Connell, C.B., Wheatley, S.P., Ahmed, S., and Wang, Y.-L. (1999). The small GTP-binding protein Rho regulates cortical activities in cultured cells during division. J. Cell Biol. *144*, 305–313.

Pelham, R.J., Jr., and Wang, Y.-L. (1997). Cell locomotion and focal adhesions are regulated by substrate flexibility. Proc. Natl. Acad. Sci. USA *94*, 13661–13665.

Pelham, R.J., Jr., and Wang, Y.-L. (1999). High resolution detection of mechanical forces exerted by locomoting fibroblasts on the substrate. Mol. Biol. Cell *10*, 935–945.

Robinson, D.N., and Spudich, J.A. (2000). Towards a molecular understanding of cytokinesis. Trends Cell Biol. *10*, 228–237.

Rochlin, M.W., Itoh, K., Adelstein, R.S., and Bridgman, P.C. (1995). Localization of myosin II A and B isoforms in cultured neurons. J. Cell Sci. *108*, 3661–3670.

Saitoh, T., Takemura, S., Ueda, K., Hosoya, H., Nagayama, M., Haga, H., Kawabata, K., Yamagishi, A., and Takahashi, M. (2001). Differential localization of non-muscle myosin II isoforms and phosphorylated regulatory light chains in human MRC-5 fibroblasts. FEBS Lett. *509*, 365–369.

Sheetz, M.P., Felsenfeld, D.P., and Galbraith, C.G. (1998). Cell migration: regulation of force on extracellular-matrix-integrin complexes. Trends Cell Biol. *8*, 51–54.

Shestakova, E.A., Singer, R.H., and Condeelis, J. (2001). The physiological significance of $\beta$-actin mRNA localization in determining cell polarity and directional motility. Proc. Natl. Acad. Sci. USA *98*, 7045–7050.

Simons, M., Wang, M., McBride, O.W., Kawamoto, S., Yamakawa, K., Gdula, D., Adelstein, R.S., and Weir, L. (1991). Human nonmuscle myosin heavy chains are encoded by two genes located on different chromosomes. Circ. Res. *69*, 530–539.

Small, J.V. (1981). Organization of actin in the leading-edge of cultured cells. Influences of osmium tetroxide and dehydration on the ultrastructure of actin mesh works. J. Cell Biol. *91*, 695–705.

Svitkina, T.M., Verkhovsky, A.B., McQuade, K.M., and Borisy, G.G. (1997). Analysis of the actin-myosin II system in fish epidermal keratocytes: mechanism of cell body translocation. J. Cell Biol. *139*, 397–415.

Totsukawa, G., Yamakita, Y., Yamashiro, S., Hartshorne, D.J., Sasaki, Y., and Matsumura, F. (2000). Distinct roles of ROCK (Rho-kinase) and MLCK in spatial regulation of MLC phosphorylation for assembly of stress fibers and focal adhesions in 3T3 fibroblasts. J. Cell Biol. *150*, 797–806.

Tullio, A.N., Accili, D., Ferrans, V.J., Yu, Z.-X., Takeda, K., Grinberg, A., Westphal, H., Preston, Y.A., and Adelstein, R.S. (1997). Nonmuscle myosin IIB is required for normal development of the mouse heart. Proc. Natl. Acad. Sci. USA *94*, 12407–12412.

Uren, D., Huang, H.K., Hara, Y., Takeda, K., Kawamoto, S., Tullio, A.N., Yu, Z.X., Ferrans, V.J., Tresser, N., Grinberg, A., Preston, Y.A., and Adelstein, R.S. (2000). Gene dosage affects the cardiac and brain phenotype in nonmuscle myosin II-B-depleted mice. J. Clin. Inv. *105*, 663–671.

Wang, Y.-L., and Pelham, Jr., R.J. (1998). Preparation of a flexible porous polyacrylamide substrate for mechanical studies of cultured cells. Methods Enzymol. *298*, 489–496.

Wei, Q., and Adelstein, R.S. (2000). Conditional expression of a truncated fragment of nonmuscle myosin IIA alters cell shape but not cytokinesis in HeLa cells. Mol. Biol. Cell *11*, 3617–3627.

Wessels, D., Soll, D.R., Knecht, D., Loomis, W.F., DeLozanne, A., and Spudich, J.A. (1988). Cell motility and chemotaxis in *Dictyostelium* amebae lacking myosin heavy chain. Dev. Biol. *128*, 164–177.

Wolenski, J.S. (1995). Regulation of calmodulin-binding myosins. Trends Cell Biol. *5*, 310–316.

Wylie, S.R., Wu, P.-J., Patel, H., and Chantler, P.D. (1998). A conventional myosin motor drives neurite outgrowth. Proc. Natl. Acad. Sci. USA *95*, 12967–12972.

Wylie, S.R., and Chantler, P.D. (2001). Separate but linked functions of conventional myosins modulate adhesion and neurite outgrowth. Nat. Cell Biol. *3*, 88–92.